

Analysis of Ion Flow Field of UHV/EHV AC Transmission Lines

Bo Zhang, Wei Li, Jinliang He and Rong Zeng

Tsinghua University
State Key Lab of Power Systems, Department of Electrical Engineering
Beijing 100084, China

ABSTRACT

In this work, the calculation method of the ion flow field of AC transmission lines based on the charge simulation method is improved. As the previous works, the problem is solved in time domain with representing the space charges as discrete line charges. In each discrete time step, the procedures of charge emission, space charge displacement, and space charge recombination are simulated. As improvements, the influence of the conductor surface field uniformity on corona discharge is taken into account, so that the ion flow field of multi-phase or bundle conductors can be simulated in this work. The corona losses of a 3-phase 8-conductor bundle HVAC transmission line is calculated. Acceptable agreement is obtained with the experimental results. The ground level total electric field of different line configurations is calculated. The influences of line configurations such as subconductor radius, bundle spacing, number of subconductors, wire spacing, and phase height on ground level total electric field are analyzed based on the calculation.

Index Terms - Corona, electric fields, Space charge, simulation, transmission lines.

1 INTRODUCTION

THE corona phenomenon is an important issue of HV power transmission lines. When the electric field in the near vicinity of a HV conductor exceeds the breakdown strength of the air, a small volume of the air surrounding the conductor is broken down. The discharge results in the production of positive ions and negative charges (ions and electrons). Charges of opposite polarity to that of the conductor move towards it and may be neutralized on the conductor surface. Charges of the same polarity of the conductor move away from it towards the ground or the other conductors. Therefore, the conductor appears to emit charges, called space charges [1, 2]. On AC transmission lines, the space charges created by the corona are constrained to the near vicinity of the conductor because of the periodic reversal of the electric field [3-5]. The movement of the space charges consumes energy of power lines, called corona losses. Furthermore, the space charges may affect the space electric field, even on the ground level.

Efforts have been made on the experimental research of AC corona losses. The experiments performed on corona cages or test lines indicated that the subconductor radius, phase height, wire spacing, and conductor surface condition all affect the corona losses [6-11].

Systematic experiments have been performed by EPRI in 1970s. Empirical formula for AC corona losses has been

obtained by fitting the experimental results. However, the application range of this formula is limited due to the lack of theoretical foundation [12].

Clade et al. proposed a method for calculating AC corona losses in the coaxial cylinders configuration based on constant electric field at the conductor with corona [13-16]. Actual measurements of corona onset field, corona losses, and corona current in a small corona cage were taken to validate their calculation method [17, 18]. However, the space charges are considered not altering the field direction in this method. So the calculation proceeds in one dimensional path along the space-charge-free electric field (the electric field due to the charges in the conductors, excluding the effect of the space charge present in the interelectrode space) lines, which is suitable only for coaxial cylinders configuration. However, for nonsymmetrical structures, such as line-to-plane structure, the space charges affect the field direction actually. Clade's method will introduce unacceptable errors due to the deviation between the directions of the total electric field and the space-charge-free electric field.

Abdel-Salam calculated the corona losses for line-to-plane structure with a charge simulation method (CSM) based method. Satisfactory agreement was obtained between calculated result and experimental result for both single-phase and 3-phase single-conductor situations [19-21]. The quantity of charges emitted from conductor was calculated based on the definition of 'corona onset charge'. The ion flow field has been calculated by applying the point form of Gauss law in the space charge shells which was

justified near the conductor with corona. The difference of the corona discharge caused by different field strength at different position on conductor surface is neglected. So this method is not applicable for actual bundle conductor of HVAC transmission lines due to the remarkable field difference on the conductor surfaces. In [22], a finite volume-based approach for the hybrid ion-flow field of UHVAC and UHVDC transmission lines in parallel is put forward. It can take the actual bundle conductor of HVAC transmission lines into account. But the method is complex and the calculation speed is very slow compared with Salam's method because the whole space takes part in the calculation.

Meanwhile, the issue of corona losses has been a research focus for a long time. However, the corona effect on electric field of HVAC lines is usually neglected due to the common sense that the movement of the space charges is constrained. That is, the corona effect is left out of account in the calculation of ground level electric field when designing HVAC transmission lines. But at present, there is a lack of calculating or experimental research on the ground level electric field effect caused by corona discharge for the ultra-high voltage (UHV) and extra-high voltage (EHV) AC transmission lines. Quantitative research should be taken on this problem.

This work improves the CSM based AC corona losses calculation method proposed by Salam. The major contribution is the new processing methods on corona onset criterion and charge emission. The influence of the conductor surface field uniformity on corona discharge is taken into account, so that the ion flow field of multi-phase or bundle conductors can be simulated. The details of the computational method are described at first. Then, the characteristics of the corona losses on HVAC lines are discussed. At last, the influences of line configurations on ground level electric field are analyzed.

2 COMPUTATIONAL METHOD

2.1 PROCESS OVERVIEW

The first step of AC ion flow field simulation is to calculate the corona onset charge based on Kaptzov's assumption without regard to the space charges. Then, the alternating cycle is divided into discrete time steps. In each step, the quantity of the simulation charges is compared with the quantity of the corona onset charge on the conductor surface. Corona discharge takes place if the former is greater. And a certain quantity of charge is emitted from conductor to space. The space charges migrate with the electric field force and reduce with the recombination effect. This calculating procedure is carried out cyclically and continuously until the termination criterion is met. Then, corona parameters as corona losses, corona current and ground level total electric field can be gained with further calculation.

Figure 1 is the flow chart of the procedure of the AC ion flow field simulation. This procedure is similar to the one for single conductor configuration proposed in [19]. To move forward, improvements have been made for corona onset criterion and charge emission, which are included in step 1-4 in Figure 1.

2.2 CALCULATION OF THE ONSET CHARGE

The total field on a conductor surface with corona is considered to be maintained at the onset value in Kaptzov's assumption [13-16, 19-21]. However, the charges emitted from conductor are difficult to be deduced directly from this assumption on field value. For this reason, the concept of corona onset charge was introduced in [19]. In [19], the CSM was used to solve the space-charge-free field problem. The simulation charge was set in the vicinity of the inner surface around the conductor. The corona onset charge was defined as the total simulation charge in the conductor when the maximum surface field exceeds the onset value. The corona onset charge was assumed time-invariant, so it was calculated once for all. Then in each time step, the conductor simulation charge is calculated considering both the conductor induced and the space charge induced electric potential. If the total conductor simulation charge exceeds the corona onset charge, the corona discharge occurs. The excess charge is emitted to space evenly around the conductor surface.

Actually, the electric field on conductor surface is affected by the space charges around it. So the corona onset charge should not be calculated only with conductor electric potential while the space charges exist. On the other hand, the electric field distributes nonuniformly on conductor surface of unsymmetrical structures as actual power transmission line structures, especially for bundle conductors. It is unreasonable to assume corona discharge occurs uniformly around the conductor. So in [19], the bundle conductor was represented by single conductor with equivalent radius to get around this question. And unacceptable errors were introduced when different phases close to each other.

In this work, the conductors are also discrete as several simulation line charges, as Figure 2. But the corona onset charge is defined at each discrete point where the simulation line charge is located rather than a total value and is calculated respectively. The new definition of corona onset charge at a single point is the simulation charge of this point when the applied voltage makes the surface field near this point just equal to the onset field. The effects induced by space charges is taken into account, so the calculation of corona onset charge processes in the beginning of each time step, as the dotted line indicated in Figure 1.

The numerical method is described concisely with the example of single conductor AC ion flow field calculation. The simulation charges are set in the vicinity of the inner surface around the conductor, while the matching points are set on the conductor surface just above the simulation charges, and one matching point to one simulation charge, as Figure 2 indicated. If the number of the simulation charges is M , the number of the space charges is N (because of charge emission and recombination, N is a time dependent variable), the corona onset charge of point r inside the conductor can be calculated as follows.

The following equations are satisfied when the electric field at matching point r' meets the onset value:

$$P_{cond} \cdot Q_{cond} + P_{space} \cdot Q_{space} = V_{onset} \quad (1)$$

$$R_{cond,r'} \cdot Q_{cond} + R_{space,r'} \cdot Q_{space} = E_{onset} \quad (2)$$

Equation (1) represents the electric potential contribution to the matching points by the simulation charges and the space charges. $\mathbf{P}_{cond}(M \times M)$ represents the potential coefficient matrix between the simulation charges and the matching points. $\mathbf{P}_{space}(M \times N)$ represents the potential coefficient matrix between the space charges and the matching points. $\mathbf{Q}_{cond}(M \times 1)$ represents the simulation charge vector. $\mathbf{Q}_{space}(N \times 1)$ represents the space charge vector. $\mathbf{V}_{onset}(M \times 1)$ represents the conductor potential when the field at matching point r' just meets the onset value. The values of elements in \mathbf{V}_{onset} are equal because the surface of a conductor is equipotential.

Equation (2) represents the electric field contribution to matching point r' by the simulation charges and space charges. $\mathbf{R}_{cond, r'}(1 \times M)$ represents the field coefficient matrix between simulation charges and matching point r' . $\mathbf{R}_{space, r'}(1 \times N)$ represents the field coefficient matrix between space charges and matching point r' . E_{onset} is the corona onset field, which can be calculated with Peek's equation [18].

The equations (1) and (2) have $(M+1)$ equations. If the value of \mathbf{Q}_{space} is considered as known variable, then by solving equations (1) and (2) simultaneously, the $(M+1)$ unknown variables in both \mathbf{Q}_{cond} and \mathbf{V}_{onset} are obtained. The r -th element $Q_{cond, r}$ of \mathbf{Q}_{cond} is the corona onset charge of point r .

For each point where a simulation charge is located, there is a corresponding corona onset charge. At each point, by substituting equation (2) with a new equation, the corresponding corona onset charge can be obtained. The process of solving corona onset charge is taken on every points where the simulation charges are located. Then, the onset charge vector \mathbf{Q}_{onset} for all the points is set up. By considering both positive and negative polarity corona discharge, onset charge $\mathbf{Q}_{onset\pm}$ is solved.

For bundle conductors and transmission lines, the simulation charges are in all the subconductors. For each point where a simulation charge is located, there is also a corresponding corona onset charge, which can also be obtained by above method if all the coefficient matrices are set up by taking account of the relationship between all the charges and the matching points.

In practice, it is found that 12 simulation line charges in each subconductor were enough to simulate the electric field near the conductor. In all the following cases, the number of the simulation line charges in each subconductor is fixed at 12.

2.3 CALCULATION OF CHARGE EMISSION

Charge emission is an important issue in this calculation method. In this work, corona onset judgment and charge emission calculation are proceeded at every surface points. At each time step, simulation charge \mathbf{Q}'_{cond} and corona onset charge $\mathbf{Q}_{onset\pm}$ are calculated. The elements of the two vectors are compared. If $Q'_{cond, r} > Q_{onset+, r}$ or $Q'_{cond, r} < Q_{onset-, r}$, corona discharge occurs on point r , and the exceeded charge is emitted in to space.

The calculation process of $\mathbf{Q}_{onset\pm}$ has been introduced in section 2.2. The calculation process of \mathbf{Q}'_{cond} is as follows.

The alternating cycle is divided into NT discrete time steps. At step i , the voltage applied on conductor is:

$$V_{app} = V_{max} \sin[\omega(i-1)\Delta t] \quad (3)$$

where, $i=1, 2, 3, \dots, NT$. Usually each cycle can be divided into 100 steps which represents a good compromise between the accuracy and the computational time.

The conductor is represented by M simulation line charges. Equation (4) is satisfied at the matching points.

$$\mathbf{P}_{cond} \cdot \mathbf{Q}'_{cond} + \mathbf{P}_{space} \cdot \mathbf{Q}_{space} = V_{app} \quad (4)$$

where, \mathbf{P}_{cond} and \mathbf{P}_{space} have the same meaning as equation (1), $V_{app}(M \times 1)$ is the applied voltage at the present step. With equation (4) simulation charge vector \mathbf{Q}'_{cond} can be obtained.

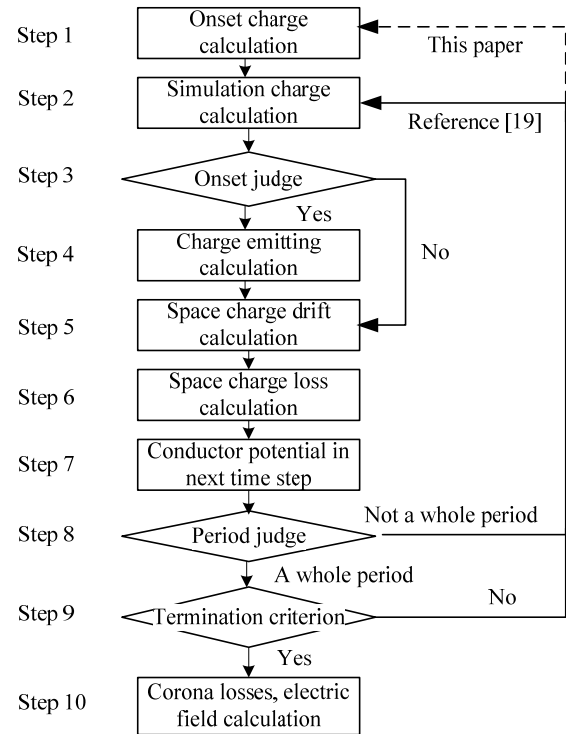


Figure 1. Flow chart of AC corona losses calculation.

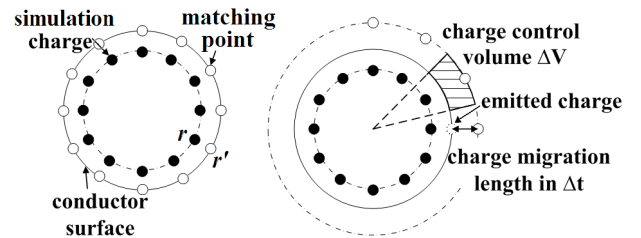


Figure 2. Charge emission process.

2.4 SPACE CHARGE DISPLACEMENT

The space charges with the same polarity of voltage are pushed away, while the opposite ones are pulled nearer. The

displacement Δd of a charge in time interval Δt is [20]:

$$\Delta d = \mu E \Delta t \quad (5)$$

where, μ is ion flow mobility, $1.5 \times 10^{-4} \text{ m}^2/\text{V}\cdot\text{s}$ for positive charge and $1.8 \times 10^{-4} \text{ m}^2/\text{V}\cdot\text{s}$ for negative charge. E is the total field calculated with CSM.

2.5 SPACE CHARGE LOSS

The movement of space charges is described by equation (5). The charge will be neutralized and disappear from analysis when it reaches the conductor surface.

Positive and negative space line charges meet in the space, and recombine. For the calculation of the recombination, the volume occupied by each charge is defined by the location of the charge in two successive time steps, as Figure 2. Positive and negative charge densities are expressed as:

$$\rho_{\pm} = \frac{q_{\pm si}}{e \Delta V_i} \quad (6)$$

where, ΔV_i is the volume associated with the charge. $q_{\pm si}$ is the positive or negative space charge. $e = 1.6 \times 10^{-19} \text{ C}$ is the electron charge.

Then the recombination process can be expressed as [20]:

$$q_{\pm si, t+\Delta t} = \frac{q_{\pm si, t}}{1 + |\gamma \Delta t \rho_{\pm}|} \quad (7)$$

where, $\gamma = 1.5 \times 10^{-12} \text{ m}^2/\text{s}$ is the recombination coefficient.

The quantity of space charges declines due to the recombination effect. In this paper, the maximum charge density in the process of calculation is recorded. If the charge density is smaller than 0.01% of the maximum value, it will be removed from the calculation process.

2.6 TERMINATION CRITERION

Because the calculation starts with the initial value without regard to the space charges, the computational stability will be reached after several alternating cycles.

The total space charge is recorded in each time step:

$$q_{space, sum} = \sum_{i=1}^N q_i \quad (8)$$

The total space charge generated in one period is

$$q_{cycle, sum} = \sum_{j=1}^{NT} q_{space, sum, j} \quad (9)$$

The computational stability is considered to be achieved if the change of $q_{cycle, sum}$ between two adjacent periods is less than a certain value. That means:

$$\left| \frac{q_{cycle, sum, N_c} - q_{cycle, sum, N_c-1}}{q_{cycle, sum, N_c-1}} \right| < \varepsilon \quad (10)$$

where, N_c represents the present period. ε represents the error tolerance.

According to the calculation results, the error of $q_{cycle, sum}$ is usually less than 1% after a calculation time of 10 periods. Thus, in this paper, ε is 1%.

2.7 CALCULATION OF CORONA LOSSES, CORONA CURRENT AND GROUND LEVEL TOTAL ELECTRIC FIELD

The energy consumed by the migration of space charges is supplied by the conductor. The energy loss caused by corona effect is defined as corona losses [20].

The displacement Δd of the i -th charge in time interval Δt is:

$$\Delta d_i = \mu E_i \Delta t \quad (11)$$

The energy consumed is:

$$W_i = q_i E_i \cdot \Delta d_i \quad (12)$$

The total energy consumed in one period is:

$$W = \int_{\text{cycle } N} \sum q_i E_i \cdot \Delta d_i \quad (13)$$

The average power in this period is:

$$P = fW \quad (14)$$

where, f is AC frequency.

The corona current contains two parts: The displacement current i_{displ} can be represented by the change of conductor charges. The conductive current i_{conv} is related to the migration of space charges. In i_{displ} , the capacitive current i_{cap} without regard to the corona discharge should be removed [19].

$$i_{displ} = \frac{\Delta \sum q_{cond}}{\Delta t} \quad (15)$$

where, q_{cond} represents the conductor charges considering corona effect.

$$i_{cap} = \frac{\Delta \sum q_{cond, norm}}{\Delta t} \quad (16)$$

where, $q_{cond, norm}$ represents the conductor charges without regard to corona effect.

$$i_{conv} = \sum_N \frac{q_{space} \mu_{\pm} E_s^2}{V_{app}} \quad (17)$$

where, q_{space} represents the space charges. E_s represents the value of the field on the position of space charges. V_{app} represents the applied voltage at present.

The total corona current is:

$$i_{cor} = i_{displ} - i_{cap} + i_{conv} \quad (18)$$

The electric field on spatial point p can be calculated as follows:

$$\vec{E}_p = \sum_{i=1}^M R_{p,i} q_i + \sum_{j=1}^N R_{p,j} q_j \quad (19)$$

On the right-hand-side of this equation, the first part represents the field contribution by the conductors, while the second part represents the field contribution by the space charges.

3 CORONA LOSSES ANALYSIS

3.1 CORONA LOSSES AND CURRENT ANALYSIS OF A SINGLE CONDUCTOR

Paper [20] provides the simulating and experimental results of corona losses on a single conductor line-to-plane structure, the corona losses difference associated with the applied voltage is analyzed. The radius of the conductor is 3.28 mm, and the height is 2.59 m. The results are illustrated as Figure 3, where curve A and curve B are the experimental result and the calculated result respectively in [20] with conductor roughness factor of 0.7, curve C is the calculated result in our work with the same roughness factor as curve B. The results indicated that the new approach is better than the previous one. The reason of comparatively large difference between the heads of the curves is because the corona discharge incepts suddenly when the onset value is exceeded in the calculation process. However, the surface of conductor is usually not smooth in practical terms, the corona discharge occurs on random irregular points rather than on all surface points due to the higher field value at relatively low voltage level. This makes the change of losses gentler at relatively low voltage level for the experimental result than the calculated result. Because curve C takes space charge into account when calculating corona onset charge whereas curve B neglects space charge effect, more satisfactory agreement is obtained between calculated result and experimental one for curve C.

The calculated result indicated that for this single conductor, 99% of the space charges are concentrated in a small range no more than 0.24 m from the line center. This distance is about 73 times of the subconductor radius, which is consistent with the conclusion that the maximum charge displacement distance is about 70 times of the subconductor radius in [13].

Figure 4 illustrated the calculated corona current waveform with applied voltage of 75 kV. Curve A represents the calculated corona current. Curve B represents the phase of applied voltage. Curve C represents a sketch of corona current in theory [1]. The calculated waveform is similar to the theoretical one.

3.2 CORONA LOSSES OF MULTIPHASE BUNDLE CONDUCTORS

The corona losses of field asymmetry structures such as multiphase bundle conductors can be analyzed with this method. An actual 3-phase HVAC transmission line proposed in [12] is used as an example. The phase height H is 24 m; wire spacing L is 18.5 m; number of subconductors is 8; bundle spacing D is 39 cm. Figure 5 illustrated the transmission line configuration. The voltage applied is 1200 kV. The phase sequence from left to right is A, B, and C. The corona losses for the line as a whole are measured and the influences of conductor diameter on corona losses are analyzed in [12]. Corresponding corona losses are also calculated by the method in this paper as Figure 6 shows. In

Figure 6, A is the measured result in heavy rain; B, C, D are the calculated results in this paper, where the conductor roughness factor is set 0.6, 0.65, 0.7 respectively. The calculated result with conductor roughness factor of 0.65 is closest to the experimental one, which is in accordance with the conclusion in [15] that the value of conductor roughness factor should be set between 0.5 and 0.75, increasingly with the rainfall intensity decreases.

The diameter of the subconductors in Figure 6 is just for laboratory investigation because the corona is too strong and cannot be used in reality. Following is the analysis for a transmission line with subconductor diameter of 3 cm and the conductor roughness factor of 0.65. In this case, there is no corona on the side phases because the maximal electric field on the surface of the subconductors is just beneath the onset value. The corona losses for the line as a whole is just from the central phase. Calculation in this paper shows that the corona losses are 19.61 kW/km. Figure 7 illustrates the RMS corona current emitted from subconductors of the central phase. Due to symmetry, only the results of left side subconductors of the central phase are presented. The subconductor number can be found from Figure 5. It can be seen that the the corona discharges on the subconductors is different because the electric fields on them are different. Corona discharge is stronger on the subconductors close to the ground and the other two phases.

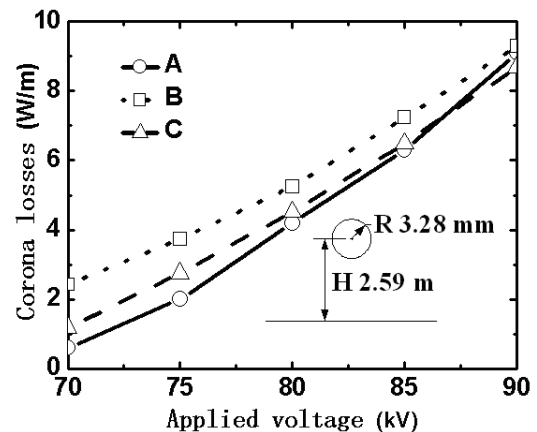


Figure 3. Corona losses calculation and experiment result of single conductor

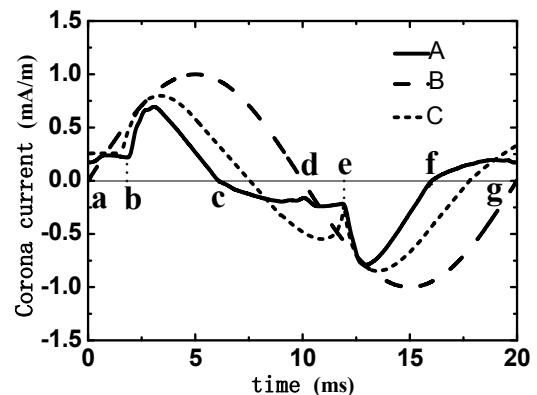


Figure 4. Waveform of corona current

Figure 8 illustrates the calculating result of space charge field intensity around the central phase with conductor roughness factor of 0.65, conductor diameter of 3cm, and voltage phase angle of 72°. The field intensely region distributes in the outer region around the conductors. That is, the corona discharges occur mostly on the side pointing outward from line center, instead of the inner side. This fact reflects the field nonuniformity around bundle conductors and confirms that the corona onset charge and charge emission calculation should be implemented respectively on different points on conductors. The calculation result indicated that, to the 3 phase 8 bundle conductors, 99% of the space charges are concentrated in a range that no more than 1.3m from the line center, that is 2.5 times to the subconductor radius.

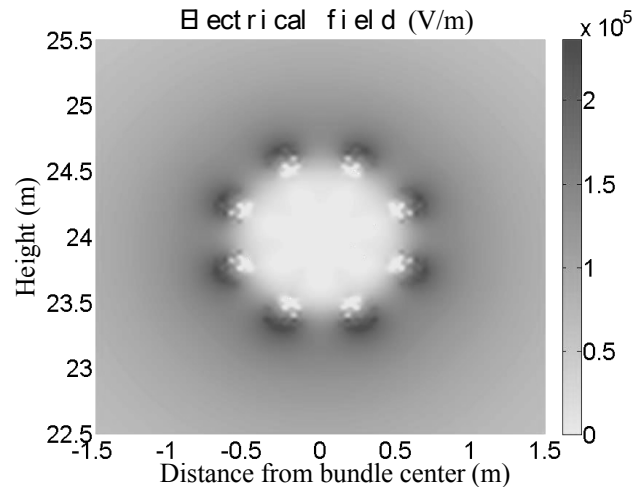


Figure 8. Electric field produced by the space charges in the vicinity of bundle conductor.

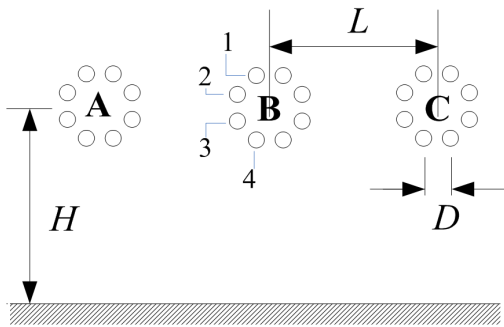


Figure 5. Configuration of the analyzed transmission line.

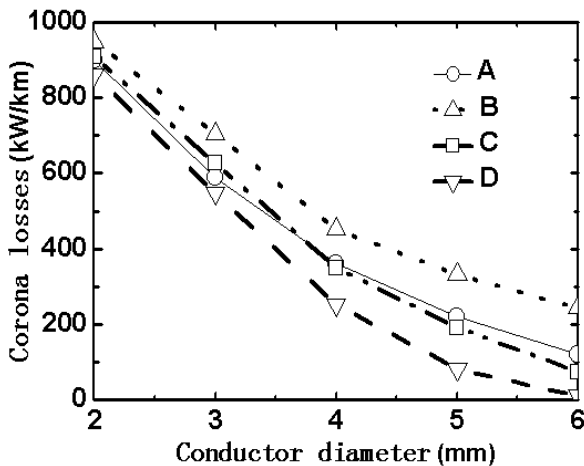


Figure 6. Corona losses for the line as a whole with different conductor diameters.

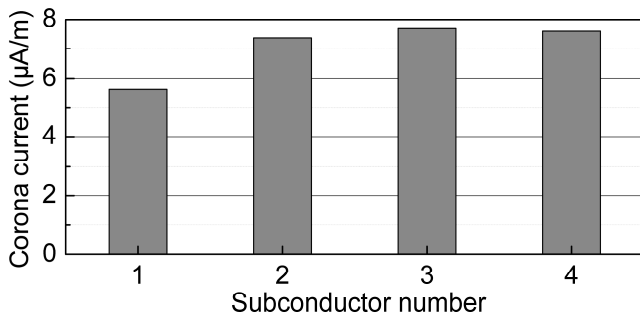


Figure 7. RMS Corona current emitted from subconductors.

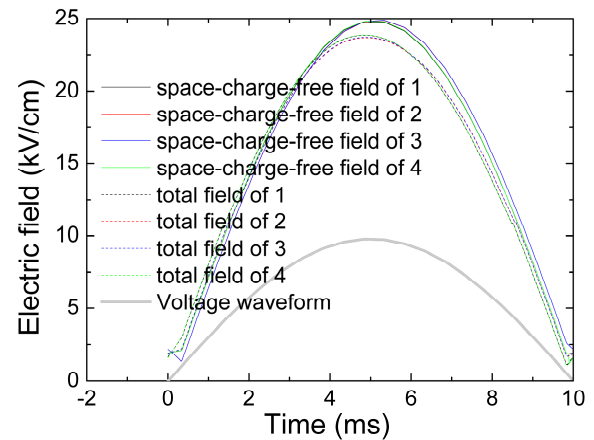


Figure 9. Temporal variation of the absolute value of the maximal electric field around the subconductors.

Figure 9 illustrates the temporal variation of the maximal electric field around the subconductors of the central phase. Due to symmetry, only the results during the half cycle is presented. It can be seen that the total electric fields are not more than the corona onset value and are smaller than the space-charge-free fields. What's more, the peak value appears at different times for the total field, space-charge-free field, and the applied voltage. The peak value of the total field appears somewhat earlier than that of the applied voltage. While the peak value of the space-charge-free field appears somewhat later than that of the applied voltage. This may be due to the effect from the other two phases and the space charges. On the subconductors, the times when the peak values appear are also different.

4 GROUND LEVEL ELECTRIC FIELD ANALYSIS

4.1 INFLUENCE OF VOLTAGE LEVELS

The influence of corona discharge on ground level electric field depends on the strength of discharge. The ground level electric field with corona effects is calculated for typical 110

kV, 220 kV, 500 kV, 750 kV, and 1000 kV HVAC transmission lines. The three phase lines are all displaced with the same height and equal space. The bundle spacing is 40 cm. In Table 1, the influence can be described by the difference between the ground level total electric field and the space-charge-free electric field.

Table 1. Typical line parameters and ground level electric field of different voltage levels.

Line voltage(kV)	110	220	500	750	1000
Phase height(m)	7	8	15	18	22
Phase space(m)	4	6	11	15	18
Subconductor number	1	2	4	6	8
Conductor cross sectional area (mm ²)	240	300	400	400	630
E_{max} (kV/m)	1.83	4.77	5.73	8.04	9.02
E_{maxn} (kV/m)	1.83	4.75	5.59	7.72	8.57
$DiffE_m$ (%)	0	0.5	2.5	4.2	5.2

E_{max} : maximum value of total field;
 E_{maxn} : maximum value of space-charge-free field;
 $DiffE_m$: maximum value difference between total field and space-charge-free field

More subconductor number and larger subconductor radius are usually employed for higher voltage level. This suppressed the corona discharge intensity to some extent. However, stronger influence of corona on ground level electric field is also found for higher voltage level transmission lines according to the calculation. So the research on the influence of corona discharge on ground level electric field of 1000 kV HVAC transmission line is necessary.

4.2 INFLUENCE OF LINE PARAMETERS

The conductor size and line arrangements affect the conductor surface electric field and consequently affect the corona losses, radio interference, audio noise, and ground level electric field.

The space-charge-free electric field and corona effect both change with the line parameters. But the trend of the change may be different. So it is difficult to analyze the changing trend of total electric field. The ion flow field of a 3 phase 1000 kV HVAC transmission line is simulated. The corona effect and electric field influence of subconductor radius, bundle spacing, subconductor number, wire spacing, and phase height are analyzed.

The three line phases are all displaced with the same height and equal space. A line of 8×630 mm² conductor, 40cm bundle spacing, 18 m wire spacing and 22 m height is appointed as the standard line of reference.

4.2.1 INFLUENCE OF SUBCONDUCTOR RADIUS ON GROUND LEVEL ELECTRIC FIELD

The calculation results with different subconductor radius are listed in Table 2. It can be concluded, with the subconductor radius increasing, the maximum space-charge-free field slightly increases while the maximum total field slightly decreases. That's because the corona discharge is more intense for smaller radius due to stronger conductor surface field. The strengthen effect of corona on ground level field is more distinctly for small subconductor radius. This altered the original changing trend of field depending on

subconductor radius. Between conductor cross sectional area range of 500 to 800 mm², the maximum total field ratio of present line and standard line changes slightly between 0.6% to -0.6%, the influence of corona effect on the maximum total field changes between 6.3% to 4.3%.

Table 2. Influences of corona effect on maximum ground level electric field with different subconductor radius.

Conductor area (mm ²)	500	630	800
E_{max} (kV/m)	9.07	9.02	8.97
$DiffE_{max}$ (%)	0.6	0	-0.6
E_{maxn} (kV/m)	8.54	8.57	8.60
$DiffE_{maxn}$ (%)	-0.4	0	0.4
$DiffE_m$ (%)	6.3	5.2	4.3

E_{max} : maximum value of total field;
 $DiffE_{max}$: maximum total field difference between present line and the standard line;
 E_{maxn} : maximum value of space-charge-free field;
 $DiffE_{maxn}$: maximum space-charge-free field difference between present line and the standard line
 $DiffE_m$: maximum value difference between total field and space-charge-free field

4.2.2 INFLUENCE OF BUNDLE SPACING ON GROUND LEVEL ELECTRIC FIELD

The calculation results with different bundle spacing are listed in Table 3. It can be concluded, with the splitting space increasing, the maximum total field and maximum space-charge-free field both increase, while the increasing rate is slightly smaller for maximum total field. That's because the corona discharge is more intense for smaller bundle spacing due to stronger conductor surface field. However, the strengthen effect by corona is so little that cannot alter the changing trend of maximum total field, but only decrease the changing rate. Between the bundle spacing range of 30 to 50 cm, the maximum total field ratio of the present line to the standard line changes slightly between -5.3% to 4.8%, the influence of corona effect on the maximum total field changes between 5.9% to 5.0%.

Table 3. Influences of corona effect on maximum ground level electric field with different bundle spacing.

bundle spacing (cm)	30	35	40	45	50
E_{max} (kV/m)	8.54	8.79	9.02	9.23	9.45
$DiffE_{max}$ (%)	-5.3	-2.6	0	2.3	4.8
E_{maxn} (kV/m)	8.07	8.33	8.57	8.80	9.01
$DiffE_{maxn}$ (%)	-5.8	-2.8	0	2.7	5.1
$DiffE_m$ (%)	5.9	5.5	5.2	5.0	5.0

4.2.3 INFLUENCE OF SUBCONDUCTOR NUMBER ON GROUND LEVEL ELECTRIC FIELD

The calculation results with different subconductor number are listed in Table 4. It can be concluded, with the subconductor number increasing, the maximum total field and maximum space-charge-free field both increase, while the increasing rate is smaller for the maximum total field. With the subconductor number of 6, 8, 10, the maximum total field ratio of present line to standard line changes between -4.3% to 4.2%, the influence of corona effect on the maximum total field changes between 8.8% to 2.9%.

Table 4. Influences of corona effect on maximum ground level electric field with different subconductor number.

subconductor number	6	8	10
E_{max} (kV/m)	8.63	9.02	9.40
$DiffE_{max}$ (%)	-4.3	0	4.2
E_{maxn} (kV/m)	7.93	8.57	9.13
$DiffE_{maxn}$ (%)	-7.5	0	6.5
$DiffE_m$ (%)	8.8	5.2	2.9

4.2.4 INFLUENCE OF WIRE SPACING ON GROUND LEVEL ELECTRIC FIELD

The calculation results with different wire spacing are listed in Table 5. It can be concluded, with the wire spacing increasing, the maximum total field and maximum space-charge-free field both increase, while the increasing rate is smaller for the maximum total field. That's because the electric field lines in the interelectrode region are extended with enlarging the wire spacing. This lowers the conductor surface field slightly. With wire spacing of 14 to 22 m, the maximum total field ratio of present line to standard line changes between -8.4% to 6.0%, the influence of corona effect on the maximum total field changes between 6.3% to 4.5%.

Table 5. Influences of corona effect on maximum ground level electric field with different wire spacing.

Wire spacing (m)	14	16	18	20	22
E_{max} (kV/m)	8.26	8.67	9.02	9.31	9.56
$DiffE_{max}$ (%)	-8.4	-3.9	0	3.2	6.0
E_{maxn} (kV/m)	7.77	8.20	8.57	8.88	9.15
$DiffE_{maxn}$ (%)	-9.3	-4.3	0	3.6	6.8
$DiffE_m$ (%)	6.3	5.7	5.2	4.8	4.5

4.2.5 INFLUENCE OF PHASE HEIGHT ON GROUND LEVEL ELECTRIC FIELD

The calculation results with different phase height are listed in Table 6. It can be concluded, with the phase height increasing, the maximum total field and maximum space-charge-free field both increase, while the increasing rate is slightly larger for the maximum total field. That's because the electric field lines between conductor and ground are extended with enlarging the phase height. This lowers the conductor surface field slightly. With phase height of 18 to 26 m, the maximum total field ratio of present line to standard line changes between 39.5% to -24.7%, the influence of corona effect on maximum total field changes between 5.4% to 5.1%.

Table 6. Influences of corona effect on maximum ground level electric field with different phase height

Phase height (m)	18	20	22	24	26
E_{max} (kV/m)	12.58	10.56	9.02	7.78	6.79
$DiffE_{max}$ (%)	39.5	17.1	0	-13.7	-24.7
E_{maxn} (kV/m)	11.94	10.03	8.57	7.40	6.46
$DiffE_{maxn}$ (%)	39.3	17.0	0	-13.7	-24.6
$DiffE_m$ (%)	5.4	5.3	5.2	5.1	5.1

5 CONCLUSION

In this paper, the calculation method of ion flow field under multi-phase bundle conductor HVAC transmission lines is improved. The influence of the conductor surface field uniformity on corona discharge is taken into account, so that the ion flow field of multi-phase or bundle conductors can be

simulated. Then, corona losses and ground level total electric field can be obtained.

The calculation result of corona losses of single conductor is compared with previous calculating and experimental works, our calculated result accords to the experimental result better than the previous one. Satisfactory agreement is found between the calculated corona current waveform and the theoretical one.

As an example, the corona losses of a 3-phase 8-conductor bundle HVAC transmission line is calculated. The calculated result agrees to the experimental one well. The calculated result indicated that heavier rainfall causes more serious corona losses. Increasing the conductor diameter can reduce the corona losses. In addition, to the 3-phase 8-conductor bundle in this work, 99% of the space charges are concentrated in a range no more than 1.3m from the line center, that is 2.5 times to the subconductor radius.

The influence of corona discharge on ground level electric field with different voltage levels is calculated. The result indicated that the corona effect enhance the ground level electric field under HVAC transmission line, though usually not so significantly. To typical 1000 kV 3-phase HVAC transmission lines, the ground level electric field enhancement caused by corona effect is about 5%.

ACKNOWLEDGMENT

This work was supported by the National Basic Research Program of China (973 Program) under grant of 2011CB2094-01.

REFERENCES

- [1] M.P. Sarma, *Corona performance of high-voltage transmission lines*, Research Studies Press LTD, New York, 2000.
- [2] J.C. Matthews and D.L. Henshaw, "Measurements of atmospheric potential gradient fluctuations caused by corona ions near high voltage power lines", *J. Electrostatics*, Vol.67, pp. 488-491, 2009.
- [3] M. Abdel-Salam, H. Anis, A.E. Morshedy and R. Radwan, *High-Voltage Engineering: Theory and Practice*, Marcel Dekker, New York, 2000.
- [4] T.D. Bracken, R.S. Senior and W.H. Bailey, "DC electric fields from corona-generated space charge near AC transmission lines", *IEEE Trans. Power Delivery*, Vol.20, No.2, pp.1692-1702, 2005.
- [5] M. Hanafy, "Characterization of the atmospheric electrical environment near a corona ion-emitting source", *Electric Power Systems Research*, Vol.79, pp. 1-7, 2009.
- [6] T.T. Nguyen and P. Peach, "Correlation between measurements and computer evaluations of corona losses in power transmission lines", 6th Int'l. Conf. Advances in Power System Control, Operation and Management, pp. 630-634, 2003.
- [7] J.G. Anderson and L.E. Zaffanella, "Project UHV Test Line Research on the Corona Performance of a Bundle Conductor at 1000 kV", *IEEE Trans. Power App. Syst.*, Vol. 91, No.1, pp. 223-232, 1972.
- [8] T. Vinh, C.H. Shih, J.V. King and W.R. Roy, "Audible Noise and Corona Loss Performance of 9-Conductor Bundle for UHV Transmission Lines", *IEEE Trans. Power App. Syst.*, Vol.104, No.10, pp. 2764-2770, 1985.
- [9] G.W. Juette and L.E. Zaffanella, "Radio Noise, Audible Noise, and Corona Loss of EHV and UHV Transmission Lines Under Rain: Predetermination Based on Cage Tests", *IEEE Trans. Power App. Syst.*, Vol. 89, No.6, pp.1168-1178, 1970.
- [10] N. Kolcio, V. Caleca, S.J. Marmaroff and W.L. Gregory, "Radio-Influence and Corona-Loss Aspects of AEP 765-kV Lines", *IEEE Trans. Power App. Syst.*, Vol. 88, No. 9, pp. 1343-1355, 1969.
- [11] V.L. Chartier, D.F. Shankie and N. Kolcio, "The Apple Grove 750-kV Project: Statistical Analysis of Radio Influence and Corona-Loss Performance of Conductors at 775 kV", *IEEE Trans. Power App. Syst.*, Vol. 89, No. 5, pp. 867-881, 1970.

- [12] J.G. Anderson, *Transmission Line Reference Book of 345 kV and Above*, Electric Power Research Institute, Palo Alto, California, USA, 1982.
- [13] J.J. Clade, C.H. Gary and C.A. Lefevre, "Calculation of Corona Losses Beyond the Critical Gradient in Alternating Voltage", *IEEE Trans. Power App. Syst.*, Vol. 88, No. 5, pp. 695-703, 1969.
- [14] J.J. Clade and C.H. Gary, "Predetermination of Corona Losses Under Rain: Experimental Interpreting and Checking of a Method to Calculate Corona Losses", *IEEE Trans. Power App. Syst.*, Vol. 89, No. 5, pp. 853-860, 1970.
- [15] J.J. Clade and C.H. Gary, "Predetermination of Corona Losses Under Rain: Influence of Rain Intensity and Utilization of a Universal Chart", *IEEE Trans. Power App. Syst.*, Vol. 89, No. 6, pp. 1179-1185, 1970.
- [16] D.A. Rickard, J. Dupuy and R.T. Waters, "Verification of an alternating current corona model for use as a current transmission line design aid", *IEE Proc. A, Sci., Measurement and Techn.*, Vol. 138, No. 5, pp. 250-258, 1991.
- [17] K. Yamazaki, and R.G. Olsen, "Application of a corona onset criterion to calculation of corona onset voltage of stranded conductors", *IEEE Trans. Dielectr. Electr. Insul.*, Vol. 11, pp. 674-680, 2004.
- [18] D.B. Philips, R.G. Olsen, and P.D. Pedrow, "Corona onset as a design optimization criterion for high voltage hardware", *IEEE Trans. Dielectr. Electr. Insul.*, Vol. 7, pp. 744-751, 2000.
- [19] M. Abdel-Salam and D. Shamloul, "Computation of ion-flow fields of AC coronating wires by charge simulation techniques", *IEEE Trans. Electr. Insul.*, Vol. 27, No. 2, pp. 352-361, 1992.
- [20] M. Abdel-Salam and E.Z. Abdel-Aziz, "A charge-simulation-based method for calculating corona loss on AC power transmission lines", *J. Phys. D: Appl. Phys.*, Vol. 27, pp. 2570-2579, 1994.
- [21] M. Abdel-Salam and E.Z. Abdel-Aziz, "Corona power loss determination on multi-phase power transmission lines", *Electric Power Systems Research*, Vol. 58, No. 2, pp. 123-132, 2001.
- [22] H. Yin, J.L. He, B. Zhang, and R. Zeng, "Finite Volume-Based Approach for the Hybrid Ion-Flow Field of UHVAC and UHVDC Transmission Lines in Parallel", *IEEE Trans. Power Delivery*, Vol. 26, No. 4, pp. 2809-2820, 2011.



Bo Zhang (M'09) was born in Shanxi Province, P. R. China in 1976. He received his B.Sc. and Ph.D. degrees from the Department of Electrical Engineering, North China Electric Power University in Hebei, China, respectively in 1998, and 2004. He became a lecturer in the Department of Electrical Engineering, Tsinghua University in Beijing in 2005, and an associate professor in the same Department, Tsinghua University in 2008. He majors in grounding technology, EMC and EME of power system.



Wei Li was born in Tianjin, P. R. China in 1983. He received his B.Sc. and Ph.D. degrees from the Department of Electrical Engineering, Tsinghua University, Beijing, China, respectively in 2005, and 2010. Currently, he works in the Huaneng Renewables Corporation Limited. His main research interests are EME of power system and wind power generation.



Jinliang He (M'02-SM'02-F'08) was born in Changsha, China, in 1966. He received the B.Sc. degree from Wuhan University of Hydraulic and Electrical Engineering, Wuhan, China, the M.Sc. degree from Chongqing University, Chongqing, China, and the Ph.D. degree from Tsinghua University, Beijing, China, all in electrical engineering, in 1988, 1991 and 1994, respectively. He became a Lecturer in 1994, and an Associate professor in 1996, in the Department of Electrical Engineering, Tsinghua University. From 1994 to 1997, he was the Chair of High Voltage Laboratory in Tsinghua University. From 1997 to 1998, he was a Visiting Scientist in Korea Electrotechnology Research Institute in Changwon, Korea, involved in research on metal oxide varistors and high voltage polymeric metal oxide surge arresters. In 2001 he was promoted to Professor in Tsinghua University. Now he is the Chair of High Voltage Research Institute in Tsinghua University. His research interests include overvoltages and EMC in power systems and electronic systems, lightning protection, grounding technology, power apparatus, and dielectric material. He is the author of five books and 200 technical papers.



Rong Zeng (M'02-SM'06) was born in Xunyang city, Shaanxi Province, P. R. China in 1971. He received his B.Sc., M.Eng., and Ph.D. degrees from the Department of Electrical Engineering, Tsinghua University in Beijing, China, respectively in 1995, 1997, and 1999. Currently, he is the vice Dean of the Department of Electrical Engineering, Tsinghua University. He became a lecturer in the Department of Electrical Engineering, Tsinghua University in Beijing in 1999, and a professor in the same Department, Tsinghua University in 2007. His research interests include high voltage technology, grounding technology, power electronics and distribution system automation.